The Platinum Hydrido-Methyl Complex: A Frozen Reaction Intermediate?

Uwe Achatz, Martin Beyer, Stefan Joos, Brigitte S. Fox, Gereon Niedner-Schatteburg, and Vladimir E. Bondybey*

Institut für Physikalische und Theoretische Chemie, Technische Universität München, Lichtenbergstrasse 4, 85747 Garching, Germany

Received: May 20, 1999; In Final Form: August 9, 1999

Reactions of platinum−argon complexes Pt^+Ar_m, $m = 1-6$, with methane (CH_4) and methane-d_4 (CD_4) were investigated by means of FT-ICR mass spectrometry and DFT calculations. Ligand exchange reactions are observed for Pt^+Ar_m, $m = 2-6$, in which up to four argon ligands are replaced by methane. In contrast the bare platinum ion and platinum solvated with one argon ligand lead to the formation of a platinum−carbene complex. Gibbs free enthalpies from ligand exchange reactions of Pt^+CH_4 with CD_4 and H_2O provide evidence for the inserted hydrido−methyl complex HPt^+CH_3 which is corroborated by high-level DFT calculations. No isotopic scrambling is observed for the reaction of Pt^+CH_4 with CD_4 (and the reverse reaction). This is attributed to the inability of the platinum cation to form more than three covalent bonds.

Introduction

Methane activation by transition metals has been a topic of growing interest during the past decade, due to economic interest in methane conversion and chemistry. Interesting insights into the details and mechanisms of the activation process can be gained by studies of gas-phase reactions of metal ions and clusters. While several electronically excited ions were reported to form metal−carbene complexes,[1,2] thermalized ground-state monatomic transition-metal cations of the first and second row do not react with methane.[3−6] Unlike their lighter homologues, many of the third-row transition metals have been found to dehydrogenate methane exothermically, often reacting sequentially,[7,8] even though this requires a metal−carbene bond strength at least comparable to the 464 kJ/mol dissociation energy of methane to CH_2 and H_2.[9] The reaction of the M^+ (M = Ta, W, Os, Ir, Pt) cation is believed to proceed through the activation of one of the C−H bonds of methane (CH_4) and yields initially a hydrido−methyl complex, $H-M^+-CH_3$. The activation of a second C−H bond leads to a subsequent elimination of molecular hydrogen, H_2, and to the formation of the final metal−carbene complex, M^+-CH_2. Due to the considerable economical relevance of its reactions, numerous experimental and theoretical studies deal with the third-row transition-metal platinum.[7,8,10−14]

Computed energetics for the reaction of cationic platinum with methane have been reported before.[12,13] Heinemann et al.[12] computed that the insertion of platinum into the methane C−H bond proceeds with a small activation barrier of 5.4 kJ/mol. In a later publication,[13] on the other hand, the authors find the formation of the insertion product HPt^+CH_3 to be an entirely downhill process. They note that the transition state observed in geometry optimization disappears at higher levels of using both PCI-80 and B3LYP approaches. The insertion step is decisive for the methane activation, and this situation with two considerably different results for this simple reaction is therefore somewhat disturbing.

It is of interest to note that even though the monatomic second-row transition-metal cations are unreactive toward methane, we have recently shown that the same does not necessarily hold for their clusters. For example, the dimer of rhodium, Rh_2^+, reacts efficiently with CH_4 by the loss of hydrogen.[15] A recent study in our group has also shown that the presence of weakly bound argon ligands on the cluster ions has a considerable effect upon the dehydrogenation reaction.[15] Reaction of rhodium cluster argon complexes $Rh_n^+Ar_m$ with methane resulted in ligand exchange, with up to four argon atoms being replaced by a methane molecule, followed in some cases by dehydrogenation: for instance even though bare Rh_3^+ does not react with methane, Rh_3Ar^+ forms $Rh_3CH_2^+$ rather efficiently. The structure of the complexes with methane exchanged for argon without dehydrogenation is not obvious: the methane may be stabilized as an intact CH_4 molecule, or as an inserted entity such as $H-Rh_n^+-CH_3$ or as an $H_2-Rh_nCH_2^+$ complex.

The goal of the present study is to explore this question specifically for the platinum−methane system. We combine our experimental approach of cold complex formation via ligand exchange with ab initio DFT calculations to investigate the existence or lack of a barrier to metal insertion. The presence of an intact methane molecule in the $Pt^+(CH_4)$ complex would prove the existence of a barrier between the electrostatically bound platinum−methane complex, and the inserted hydrido−methyl product. To gain insight into this problem, we compare reactions of bare Pt^+ with those of the solvated Pt^+Ar_m species, and carry out a series of isotope exchange experiments.

Experimental Setup

The modified Fourier transform-ion cyclotron resonance (FT-ICR) mass spectrometer CMS47X on which the experiments were performed was decribed in detail previously.[16] Briefly, platinum argon complexes Pt^+Ar_m were produced by pulsed laser vaporization of a rotating platinum target disk (Aesar, 99.99%) with the focused 532 nm radiation of a Continuum Surelite II Nd:YAG laser (spot size on the target ~500 μm). The laser was operated at 10 Hz with 10−20 mJ in 5 ns pulses producing the initial metal plasma. The vaporization was synchronized with an argon pulse (10−20 bar, 50 μs) from a home-built piezoelectric valve. The metal plasma was entrained

10.1021/jp991665u CCC: $18.00
Published on Web 09/28/1999

in the rare gas carrier and cooled by flowing through a confining channel (30 mm, 2 mm i.d.) and subsequent supersonic expansion into high vacuum to produce solvated cluster ions of the type Pt^+Ar_m. To produce platinum−methane, platinum−carbonyl, or platinum−water clusters in the expansion, the carrier gas helium was seeded with small amounts of methane, deuterated methane, carbon monoxide, or water. The cluster ions were accelerated downstream from a 500 μm skimmer to pass the stray field of the 4.7 T superconducting magnet, transferred through four differential pumping stages into the high-field region, decelerated, and stored inside an *infinity* ICR cell.[17] Mass selection was accomplished by resonant single-frequency ejection of the unwanted ions.

The reactant gases CH_4 (Messer Griesheim, 4.5), CD_4 (Cambridge Isotope Laboratories, 99+%), and CO (Messer Griesheim, 4.7) and water were used without further purification and introduced into the ultrahigh vacuum region via a needle valve, while a constant absolute pressure of typically 10^{-8} mbar was maintained. The intensities of the mass-selected reactants and their products were recorded as a function of time. Relative reaction rates were obtained by fitting the observed time dependence of the particular cluster size concentration to the pseudo-first-order reaction kinetics and were put on an absolute scale with the accurate reactant pressure.

For the ligand exchange measurements, an additional CD_4 was admitted through a separate leak valve up to a total pressure of about 3×10^{-8} mbar. Starting from different parent ions Pt^+Ar_m, either Pt^+CH_4 or Pt^+CD_4 product complexes were produced and selected. The ongoing reactions of these complexes with CD_4 and CH_4, respectively, were recorded with varying reaction delays. Independently, we applied another method to perform the ligand exchange reactions. The platinum−methane complexes were produced in the expansion, and the mass spectra were recorded after variable reaction delays as described above.

Theoretical Method

All energies, geometries, and harmonic frequencies were computed with the B3LYP hybrid density functional method.[18,19] For all structure optimizations of Pt^+Ar_m, $m = 1-6$, the Stuttgart/Dresden effective core potentials (SECPs) were used.[20] The 60 core electrons of platinum, and the 10 core electrons of argon were replaced by the pseudopotentials. To ensure as high an accuracy as possible for the computed pathway of the reaction of Pt^+ with methane, we have used the largest available basis sets throughout the calculations. For platinum we again used the SECPs. For carbon and hydrogen the 6-311++G(3d,3dp) basis sets including diffuse and polarization functions were used for geometry optimization and energy calculation. Zero-point corrections without any scaling factor were taken from this level of theory. All computations were performed on SGI Power Challenge, DEC Alpha workstations, and Fujitsu VPP700 with GAUSSIAN 94.[21]

Experimental Results

The production of the Pt^+Ar_m clusters could be optimized by varying the source conditions and transferring parameters to change the cluster distribution. A maximum number of six argon ligands could be clustered on Pt^+ in our source, and over a wide range of parameters the Pt^+Ar_4 ion with four argon ligands proved to be the most abundant complex.

The dehydrogenation reaction 1 of bare Pt^+ ($m = 0$) with methane (Figure 1) to form the platinum−carbene complex Pt^+CH_2 proceeds with a rate constant of $k^{abs} = (4.6 \pm 0.3) \times 10^{-10}$ cm^{-3} s^{-1}, somewhat slower than the previously reported value of 8.2×10^{-10} cm^{-3} s^{-1}.[22] The difference is most likely due to differences in pressure calibration. The reaction exhibits an appreciable isotopic effect, with the corresponding rate constant for the deuterated methane, CD_4, being $(2.5 \pm 0.3) \times 10^{-10}$ cm^{-3} s^{-1}.

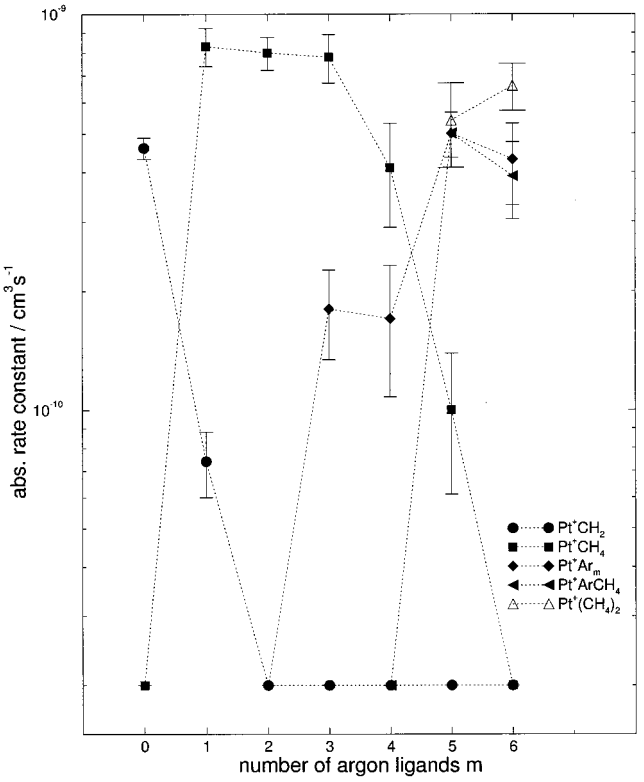

Figure 1. Absolute rate constants for the reaction of Pt^+Ar_m, $m = 0-6$, with methane. Pressure in the cell region typically 10^{-8} mbar. Rate constants denoted by hollow symbols are obtained from subsequent collisions.

Already the presence of a single argon ligand on the platinum ($m = 1$) reduces the rate of the dehydrogenation reaction 1 by more than a factor of 5 to $(7.4 \pm 1.4) \times 10^{-11}$ cm^{-3} s^{-1} for methane and $(4.2 \pm 1.4) \times 10^{-11}$ cm^{-3} s^{-1} for deuterated methane. A competing, an order of magnitude more efficient ligand exchange reaction 2, with $m = 1$ and $n = 0$, emerges:

$$Pt^+Ar_m + CH_4 \rightarrow Pt^+CH_2 + H_2 + Ar_m \qquad m = 0, 1 \quad (1)$$

$$\rightarrow Pt^+Ar_nCH_4 + Ar_{m-n} \qquad m = 1-6,\ n = 0, 1 \quad (2)$$

$$\rightarrow Pt^+Ar_{m-1} + CH_4 + Ar \qquad m \geq 3 \quad (3)$$

For platinum solvated with more than one argon ligand the methane dehydrogenation with carbene formation is not observed at all. The Pt^+Ar_m, $m = 1-6$, complexes are able to stabilize Pt^+CH_4 by ligand exchange reactions, and for $m \geq 2$ only the ligand exchange and fragmentation reactions 2 and 3 are observed. The number of ligands lost in the exchange is not quite arbitrary; for Pt^+Ar_m, $m = 1-4$, a single methane molecule replaces all the argon ligands. The dominant channel for Pt^+ solvated with five argon atoms is reaction 2, forming the Pt^+ArCH_4 complex. No complete argon loss is observed for $m = 6$, and Pt^+ArCH_4 is the only ligand exchange product. Starting with $m = 3$, also the fragmentation reaction 3 is observed, besides ligand exchange, and for $m = 5$ and in particular 6 this is the prevailing channel.

TABLE 1: Absolute Rates and Errors of the Ligand Exchange Reaction of Platinum−Argon Complexes Pt^+Ar_m, $m = 0-6$, with Methane and Methane-d_4 and the Collision-Induced Fragmentation of the Platinum−Argon Complexes Pt^+Ar_m to Pt^+Ar_{m-1}

	Pt	$PtAr_1$	$PtAr_2$	$PtAr_3$	$PtAr_4$	$PtAr_5$	$PtAr_6$
Pt^+CH_2	4.6 ± 0.3	0.7 ± 0.1					
Pt^+CD_2	2.5 ± 0.3	0.4 ± 0.1					
Pt^+CH_4		8.3 ± 0.9	8.0 ± 0.8	7.8 ± 1.1	4.1 ± 1.2	1.0 ± 0.4	
Pt^+CD_4		8.7 ± 1.4			3.4 ± 1.1		
fragm $m \rightarrow m-1$				1.8 ± 0.5	1.7 ± 0.6	5.0 ± 0.7	4.3 ± 1.0
					2.3 ± 0.4[b]		
Pt^+ArCH_4					< 0.02	5.0 ± 0.7	3.9 ± 0.9

[a] All values are in 10^{-10} cm^3 s^{-1}. [b] Fragmentation with CD_4 as collision partner.

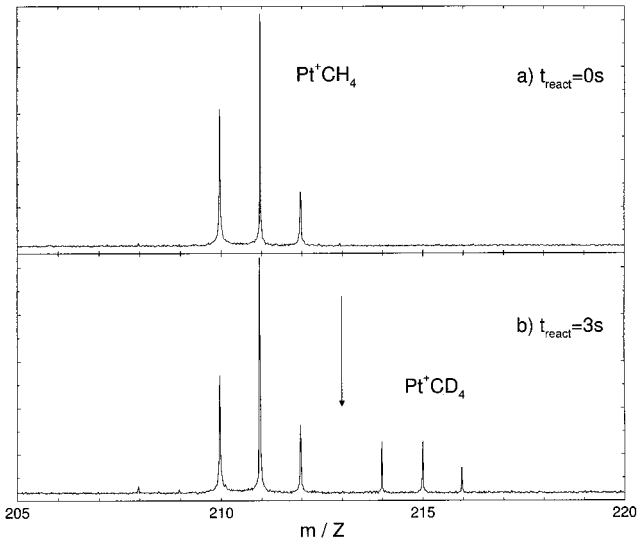

Figure 2. Part of the mass spectra for the ligand exchange reaction 4. Without reaction delay only the three selected platinum−methane peaks are in spectrum a. After a reaction delay of 3 s (b) another triple is in the spectrum with no peak at 213 amu, denoted by a downward pointing arrow (see the text).

Interesting is the fate of the mixed Pt^+ArCH_4 complex. This is able to "evaporate" the remaining argon atom, and stabilize a second methane molecule to form $Pt^+(CH_4)_2$. The measured rate constants of the reaction Pt^+Ar_m, $m = 1-6$, with CH_4 are summarized in Table 1.

To test whether methane is present in a molecular form, or decomposed by the transition metal, a variety of ligand exchange experiments were performed. Taking advantage of the ligand exchange with the platinum−argon complexes, the Pt^+CH_4 or Pt^+CD_4 ions were first generated. In the second reaction step, the ligand exchange reactions of these species with methane, methane-d_4, water, or carbon monoxide were investigated. In an alternative experiment, the platinum complexes with methane, water, or carbon monoxide were also produced directly in the expansion, simply by seeding a small concentration of the ligand species into the carrier gas.

The result of such a typical experiment in which both CH_4 and CD_4 were simultaneously introduced into the ultrahigh vacuum region is shown in Figure 2. The total absolute pressure was maintained constant around typically 10^{-8} mbar, and ligand exchange with Pt^+Ar_m, $m = 2-4$, was used to generate Pt^+CH_4 or Pt^+CD_4. After a sufficient quantity of the products had been formed, the desired species were selected by ejecting all the unwanted ions from the cell. Thus, in the experiment in Figure 2, all the remaining argon cluster "reactants" were ejected, and for clarity also the complex of the heaviest isotope ^{198}Pt with methane. The three peaks remaining in spectrum a correspond to complexes of the three most abundant isotopes of Pt^+ (194, 195, and 196 amu) with methane, CH_4. After an additional reaction delay of 3 s, a similar triplet shifted by four units to a higher mass is observed, corresponding to ligand exchange of CD_4 for CH_4. The same result was obtained, regardless of the specific Pt^+Ar_m cluster which was used to produce the methane complex. Overall, the methane ligand exchange proceeds without any indication of isotopic scrambling as described by reactions 4 and 5, whose quantitative rates are summarized in Table 2.

$$Pt^+CH_4 + CD_4 \rightarrow Pt^+CD_4 + CH_4 \quad (4)$$

$$Pt^+CD_4 + CH_4 \rightarrow Pt^+CH_4 + CD_4 \quad (5)$$

As noted above, the platinum−methane complexes can also be produced directly by seeding the carrier gas helium with traces of methane or its deuterated analogue, but the rates of the ligand exchange reactions 4 and 5 for complexes produced in this way are, within the experimental error, identical to those of the ions produced by ligand exchange with argon from Pt^+Ar_m, $m = 1-3$. As can be seen in Table 2, there is again a fairly strong isotopic effect, with the exchange of perdeuteriomethane for methane, reaction 5 proceeding about a factor of 3 faster than the reverse process, reaction 4. From the rate constant data of Table 2, one can extract the value of the equilibrium constant $K = k_{(5)}/k_{(4)}$, and applying the Arrhenius equation compute the difference in the Gibbs free enthalpy:

$$-\Delta G = RT \ln K = RT \ln(k_{(5)}/k_{(4)}) = 2.5 \pm 1.1 \text{ kJ/mol}$$

We have also carried out a series of reactions exchanging methane for other ligands, and vice versa. The clusters with water and CO were, as already mentioned, produced by seeding the carrier gas with traces of these species (see also Table 2):

$$Pt^+CH_4 + H_2O \rightarrow Pt^+H_2O + CH_4 \quad (6)$$

$$Pt^+H_2O + CH_4 \rightarrow Pt^+CH_4 + H_2O \quad (7)$$

$$Pt^+CH_4 + CO \rightarrow Pt^+CO + CH_4 \quad (8)$$

$$Pt^+CO + CH_4 \rightarrow Pt^+CH_4 + CO \quad (9)$$

The absolute rate constant for the forward and reverse exchange reactions of water and methane, reactions 6 and 7, are almost identical, corresponding to a very small difference in free enthalpy of only 0.16 kJ/mol. On the other hand, for the exchange reaction of carbon monoxide with the platinum−methane complex, reaction 8, an absolute rate constant of $k^{abs} = (1.4 \pm 0.3) \times 10^{-9}$ cm^3 mol^{-1} s^{-1} was obtained, while the reverse exchange of CH_4 with Pt^+CO, reaction 9, on the time

TABLE 2: Absolute Rate Constants for the Ligand Exchange Reaction of Pt^+CH_4 and Pt^+CD_4 with Methane, Deuterated Methane, Water, and Carbon Monoxide[a]

exchange reaction	k^{abs}	source	exchange reaction	k^{abs}	source
$Pt^+CH_4 + CD_4$	1.3 ± 0.3	expansion	$Pt^+CH_4 + CO$	14 ± 3	expansion
	1.3 ± 0.3	Pt^+Ar_2	$Pt^+CO + CH_4$	≤ 0.01	expansion
	1.3 ± 0.3	Pt^+Ar_3	$Pt^+CH_4 + H_2O$	4.7 ± 0.9	expansion
	0.7 ± 0.1	Pt^+Ar_4	$Pt^+H_2O + CH_4$	4.4 ± 1.2	expansion
$Pt^+CD_4 + CH_4$	3.7 ± 0.5	expansion	$Pt^+CH_4 + CO_2$	≤ 0.16	expansion
	3.5 ± 0.5	Pt^+Ar_2	$Pt^+CH_4 + N_2O$	≤ 0.019	expansion

[a] The source column describes the way of producing the reactants (see the text). All values are in 10^{-10} cm^3 s^{-1}.

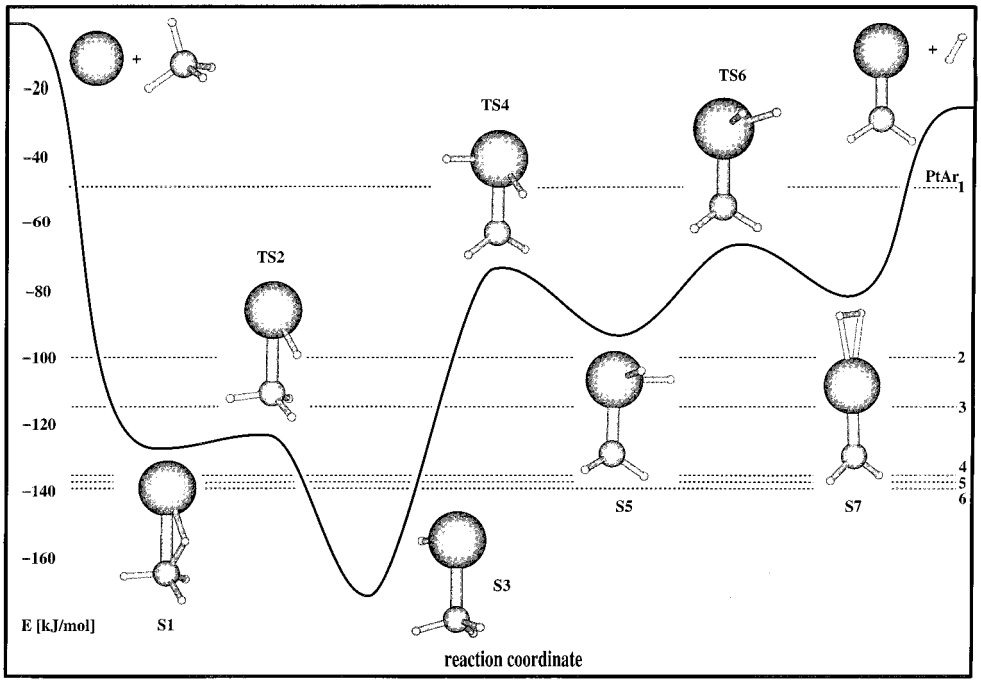

Figure 3. Calculated potential energy surface of the reaction of platinum with methane. The reaction of the Pt^+ cation proceeds through the activation of one of the C−H bonds of methane (CH_4) and yields initially a hydrido−methyl complex (HPt^+CH_3). Migration of a second hydrogen atom leads to the subsequent elimination of molecular hydrogen (H_2) to form the final metal−carbene complex M^+CH_2. The dotted lines represent the energies of Pt^+Ar_m, $m = 1-6$, from Table 4 (see the text).

scale of our experiment did not occur at all ($k^{abs} \leq 1.3 \times 10^{-12}$ cm^3 mol^{-1} s^{-1}, $-\Delta G \geq 17.4$ kJ/mol).

Theoretical Results

The potential energy surface of the methane reaction with Pt^+ was recently explored by several groups.[12,13] Pavlov et al.[13] used a DFT calculation proceeding in two steps. In the first step the stationary points of interest along the reaction path were located at the B3LYP level employing double-ζ effective core potential basis sets. In the second step the energies were calculated for the optimized geometries using enlarged basis sets with additional polarization functions. While in general this approach is justified and reliable, problems may arise under circumstances where the optimized equilibrium geometries are strongly basis-set-dependent. This is to be expected in general for species in which charge-induced dipole interactions are dominant, so that the geometries with and without polarization functions differ substantially. In the present problem this would involve for example the electrostatically bound Pt^+CH_4 species S1 and the transition state TS2 of Figure 3, i.e., exactly the key step in methane activation. For that reason we use in this publication the same large basis sets, SECPs and 6-311++G-(3d,3dp), including diffuse and polarization functions throughout the calculation, for both geometry optimization and the subsequent energy computation.

The newly computed potential energy surface for the dehydrogenation of methane by the platinum cation is shown in Figure 3, and the zero-point-corrected energies and structural parameters are summarized and compared with previous results in Table 3. The first step on the reaction path is the formation of an electrostatically bound doublet platinum−methane complex, Pt^+CH_4 (S1), which lies 126.02 kJ/mol below the initial Pt^+ and CH_4 reactants. The computed Pt−C distance in the complex is 2.28, and the 1.22 Å length of one of the C−H bonds, compared with the 1.09 Å value in free CH_4, indicates that it is activated by the interaction with the metal. The next step is the total cleavage of the C−H bond, resulting in the formation of an inserted hydrido−methyl compound (S3), the global minimum (−171.52 kJ/mol) on the potential energy surface. The distance between the platinum and the carbon is shortened to 2.05 Å, with a hydrogen bound to the platinum cation at a distance of 1.53 Å. The potential energy surface between the S1 complex and the S3 hydrido−methyl species in the region of TS2 is according to our calculation very flat, resulting in the insertion of the Pt^+ cation into the C−H bond of methane virtually without a barrier (2 kJ/mol). In the next step in the reaction sequence a second hydrogen atom migrates from the methyl to the platinum metal, resulting in a dihydrido−carbene (S5). In this complex the maximum number of three covalent bonds possible with the excited $5d^86s^1$ configuration

TABLE 3: Calculated Geometry Parameters and Relative Energies of the Reaction of Platinum with Methane[a]

	geometry		relative energy (kJ/mol)	
	Pavlov et al.	this work	Pavlov et al.	this work
S0			0	0
S1	$r_1 = 2.36$	$r_1 = 2.28$	−106.34	−126.02
	$r_2 = 1.83$	$r_2 = 1.71$		
TS2	$r_1 = 2.20$	$r_1 = 2.15$	−113.46	−124.08
	$r_2 = 1.61$	$r_2 = 1.58$		
S3	$r_1 = 2.06$	$r_1 = 2.05$	−162.45	−171.52
	$r_2 = 1.54$	$r_2 = 1.53$		
TS4	$r_1 = 1.93$	$r_1 = 1.92$	−59.45	−72.52
	$r_2 = 1.54$	$r_2 = 1.53$		
S5	$r_1 = 1.92$	$r_1 = 1.92$	−71.18	−93.37
	$r_2 = 1.49$	$r_2 = 1.53$		
TS6	$r_1 = 1.90$	$r_1 = 1.88$	−42.71	−66.24
	$r_2 = 1.65$	$r_2 = 1.63$		
S7	$r_1 = 1.87$	$r_1 = 1.87$	−69.50	−81.76
	$r_2 = 2.10$	$r_2 = 1.93$		
S8			−17.58	−25.45

[a] Data from Pavlov et al. are from ref 13 using the scaling scheme PCI-80. Our data are obtained from the B3LYP level of theory. r_1 denotes the distance between Pt and C and r_2 the distance between platinum and the first inserted hydrogen.

of Pt^+ has been formed. This step, requiring more than 78 kJ/mol, is followed by further rearrangements such as the formation of the dihydrogen complex of the cationic platinum carbene, $H_2Pt^+-CH_2$ (S7). The Pt−C distance is further shortened to 1.87 Å whereas the two H−Pt−H distances increase to 1.93 Å. The potential energy of the S7 complex increases to −81.76 kJ/mol. Finally the release of molecular hydrogen from the S7 complex requires 56.31 kJ/mol, resulting in an overall energy release of −25.45 kJ/mol for the methane dehydrogenation leading to the Pt^+CH_2 and H_2 final products. Recalculation of the zero-point corrections of the first two structures, S1 and S3, for perdeuterated methane results in slightly higher total energies of −169.49 and −125.13 kJ/mol, respectively.

To assist us in understanding the data and in the interpretation of the reactivity experiments, we have also computed the structures and energies of Pt^+Ar_m, $m = 1-6$, complexes, as well as those of Pt^+H_2O and Pt^+CO. All calculations were performed for doublet states, and all energies were zero-point-corrected. The computed structures are presented in Figure 4, and the results summarized numerically in Table 4.

Discussion

The argon ligands in Pt^+Ar_m have a role similar to that of a bulk low-temperature matrix: they can carry away the kinetic energy of the collision partners, as well as the heat of absorption of the methane reactant on the platinum ion, or of any reaction which may take place. By carrying away the excess energy, they enable a sustained contact between the methane and the metal, and permit the stabilization of the complex with CH_4. Evaporation of a single argon atom (binding energy 48.4 kJ/mol) may still leave enough energy in the reaction complex to form Pt^+CH_2, and the probability of stabilizing the inserted structure S3 is thus reduced (see dotted line 1 in Figure 3). With a second argon atom bound to the platinum ion ($E_B = 100.06$ kJ/mol) ligand evaporation leaves too little energy in the complex; it is now too low in energy to overcome the barrier TS4 and react to the platinum−carbene complex. This is reflected in the experimental data in Table 1: for the Pt^+Ar_m, $m = 1$, complex, both the ligand exchange and dehydrogenation channels are open, while for $m \geq 2$ only the ligand exchange channel is possible. The experimental data on the ligand exchange reactions of the platinum−argon complexes with methane are consistent with the computed energies of the complexes, and with the potential energy surface in Figure 3. The question which is more difficult to answer is whether the complex formed is inserted or not.

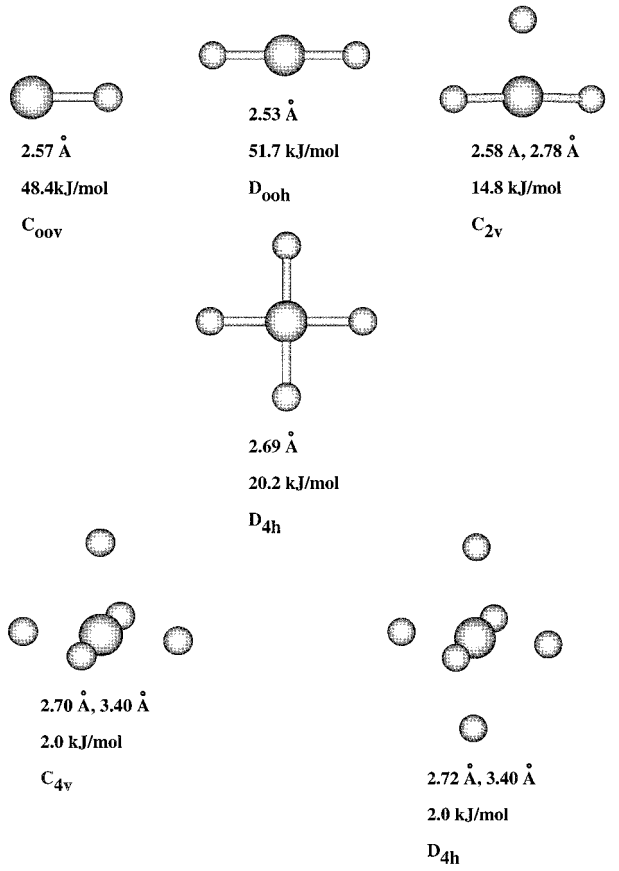

Figure 4. Calculated bond lengths and binding energies of Pt^+Ar_m, $m = 1-6$, at the B3LYP level of theory. All values are zero-point-corrected.

TABLE 4: Calculated Binding Energies and Bond Lengths of the Platinum−Argon Complexes Pt^+Ar_m, $m = 1-6$, and Relative Energies of Pt^+H_2O, Pt^+CO, Pt^+CH_4, and HPt^+CH_3 at the B3LYP Level of Theory[a]

m	symmetry	stepwise solvation energy/relative energy (kJ/mol)	Pt−Ar distance (Å)
1	$C_{\infty v}$	48.4	2.56
2	$D_{\infty h}$	51.7	2.52 (×2)
3	C_{2v}	14.8	2.57 (×2)
			2.77
4	D_{4h}	21.2	2.69 (×4)
5	C_{4v}	2.0	2.70 (×4)
			3.40
6	D_{4h}	2.0	2.72 (×4)
			3.40 (×2)
Pt^+H_2O	C_s	−179.9	
Pt^+CO	$C_{\infty v}$	−261.1	
Pt^+CH_4	C_s	−126.0	
HPt^+CH_3	C_s	−171.5	

[a] All values are zero-point-corrected.

When the results of previous computations[13] are compared with those of the present work (Table 3), several differences in the potential energy surfaces are apparent. While Pavlov et al. find no barrier between the S1 and S3 structures, a small barrier and the transition state TS2 are clearly present in our results. Also the optimized geometries for some of the stationary points

on the potential surface differ by up to 0.12 Å. Differences are found for instance for S1, TS2, and S7, whereas the geometry parameters are almost identical for S3, TS4, S5, and TS6. The origin of these differences undoubtedly lies in the relatively small basis sets used in ref 13. The long-range (e.g., α-agostic) and electrostatic (e.g., charge-induced dipole) interactions can apparently not be represented accurately enough without diffuse and polarization functions. On the other hand, structures and transition states which are bound mostly covalently are calculated almost identically in ref 13 and in this work.

The presence of the argon ligands in the Pt^+Ar_m complexes makes possible the formation of a stable complex of platinum and methane, Pt^+CH_4, but as can be seen in Table 1 and Figure 1, the efficiency of this formation decreases with m, in particular for $m > 3$. This decrease in the rate constant with m is clearly due to coordinative saturation: with an increasing number of argon ligands, it becomes more difficult for the methane to penetrate to and interact with the metal cation core.[23,24] As discussed previously, over a range of expansion conditions, the cluster distribution peaks at $m = 4$. This is a well-understood effect characteristic of the $5d^9$ ground-state configuration of the Pt^+ ion. The electron missing from the 5d shell results in a nonspherical electron density distribution, with a vacancy in the $d_{x^2-y^2}$ orbital leaving four areas of lower electron density. This permits the preferential accommodation of up to four ligands in a square planar arrangement. With four argon ligands, all these preferential "equatorial" sites are occupied, leaving only the much less favorable "polar" sites, facing the full d_{z^2} orbital. This is reflected in the drastically reduced rate constants, e.g., $(1.0 \pm 0.4) \times 10^{-10}$ cm^{-3} s^{-1} for $m = 5$ (see Table 1). For $m = 6$ the methane collision partner has no access to the metal core, and only fragmentation, but no ligand exchange, is observed.

As can be seen in Table 4, the first two Ar ligands are bound to the Pt^+ by almost identical energies (48.4 and 51.7 kJ/mol), resulting in a linear $D_{\infty h}$ complex. The incremental binding energies drop drastically for Pt^+Ar_3 and Pt^+Ar_4 to 14.8 and 20.2 kJ/mol, respectively, undoubtedly due to Ar−Ar repulsion effects. These are also reflected in the Pt^+−Ar bond lengths, which increase from 2.52 (for $m = 2$) to 2.69 Å ($m = 4$). The Pt^+Ar_1 and Pt^+Ar_2 species undergo ligand exchange with methane but no collisional fragmentation. When only two ligands in a linear arrangement are present, the collision partner can easily interact with the metal, and evaporation of the relatively strongly bound Ar ligands removes enough energy to stabilize the methane complex. For larger clusters with more weakly bound argon atoms collisional fragmentation starts to compete effectively with ligand exchange. This is in particular true for species with the very weakly bound fifth and sixth polar argon ligands. These have incremental binding energies of only 2.3 and 2.1 kJ/mol, respectively, which are also reflected in the long 3.4 Å Pt^+−Ar bonding distances. For Pt^+Ar_m, $m = 5$ and 6, the formation of Pt^+ArCH_4 also becomes feasible. A loss of four argon ligands apparently carries away enough of the excess energy to permit stabilization of the fifth one in the complex. As already noted earlier, the Pt^+ArCH_4 primary product is able to efficiently exchange in subsequent collisions with methane its remaining Ar ligand to form $Pt^+(CH_4)_2$ (see Figure 1).

The experimental equilibrium constant obtained for the Pt^+-$CH_4 + CD_4 \rightarrow Pt^+CD_4 + CH_4$ process from the rates of the forward and reverse reactions 4 and 5 yielded $-\Delta G = 2.5 \pm 1.1$ kJ/mol. This can be compared with the computed zero-point energy corrected free enthalpies (300 K), which yield $-\Delta G =$ 2.03 kJ/mol when an inserted hydrido−methyl complex is assumed (S3 in Figure 3) and a 0.89 kJ/mol value when a noninserted, electrostatically bound complex is assumed (S1 in Figure 3). Thus, the experimental result is in better agreement with the inserted structure S3, but with probably both structures lying within the combined uncertainties of the computation and the experiment.

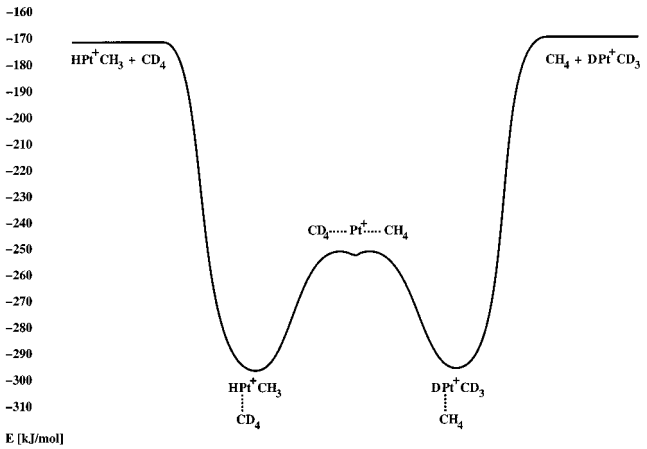

Figure 5. Estimated potential energy surface of the ligand exchange reactions 4 and 5.

Exchange reactions among labeled ligands through an inserted complex usually involve isotopic scrambling. Figure 2 displays a typical mass spectrum taken in the course of the exchange of methane against methane-d_4. Each of both species is evidenced by a triplet of peaks that reflects the isotopic composition of platinum. The moderate deviations of the relative intensities of the peaks within each triplet from those expected on the basis of natural isotopic abundances (0.97:1:0.75) are well-known to result from unwanted off-resonance excitation and space charge effects in the cell. Note, however, that the peak ratio within each of the triplets itself stays constant as the ligand exchange takes place, and there is in Figure 2b no peak at 213 amu, denoted by a downward pointing arrow, which would have been expected, if isotopic scrambling had taken place. Clearly, experimentally no isotopic scrambling takes place. This conclusion is seemingly in conflict with the computed reaction path with the inserted complex being the global minimum, and with only a minimal barrier separating it from the electrostatically bound Pt^+CH_4 complex.

This seeming contradiction between the computed reaction profile proceeding through the inserted product and the observation of no isotopic scrambling can perhaps be rationalized, if one considers in detail the electronic configuration of platinum. The Pt has a $5d^9$ ^{2}D ground state with a single unpaired d electron, but possesses a very low-lying (4786.6−16791.4 cm^{-1}) excited $5d^86s$ ^{4}F state with three singly occupied orbitals. In the inserted structure S3 two of the unpaired electrons are needed to form the covalent bonds to the hydrogen atom and the methyl ligand (Figure 3). The remaining vacancy suffices to coordinate another (e.g., perdeuterated) methane ligand in a nonclassical three-center configuration. It does not suffice, however, to allow complete activation of another C−H bond. Thus, only one bond can be activated at a time even while two methane ligands are attached to the platinum ion, and the Pt^+ cannot simultaneously insert into the C−H bonds of two methane molecules. Thus, upon colliding with a second ligand, the first methane must recombine, before the C−H bond of the incoming methane can be activated. The overall path for the methane exchange is then drawn schematically in Figure 5. The inserted HPt^+CH_3 ion

upon collision attaches a second methane (CD_4) ligand with about −125 kJ/mol binding energy. For the exchange to be completed, the system must pass through a transition state with two electrostatically bound methane ligands. This barrier corresponds effectively to the ∼45 kJ/mol recombination of the "inserted" methane, or analogue of the reverse S3 to S1 process over TS2 (see Figure 3). As noted previously, at the top of this barrier there may be a small minimum, corresponding to the small energy difference of about 2 kJ/mol computed between S1 and TS2 (Figure 3). For isotopic exchange the path in Figure 5 is not entirely symmetric, due to the minor differences in zero-point energies. The small difference of about 1 kJ/mol between inserted methane and perdeuteriomethane is responsible for the difference in rate constants in the forward and reverse reactions 4 and 5.

From the near equivalence of experimental rate constants for ligand exchange of water and methane we concluded that the binding energies of both ligands to Pt^+ should be about equal. The comparison of the computed energies of fully geometry-optimized Pt^+H_2O and Pt^+CH_4 structures yields a difference in the bond strengths of about 8 kJ/mol in favor of water. It should be noted that the relative uncertainties in computations involving entirely different species and different elements may be somewhat larger than when very similar species are compared. The obtained result is therefore in reasonable agreement with the experimental findings.

The binding energy of platinum−carbonyl was calculated to be −261.11 kJ/mol, 80 kJ/mol higher than for the bonds to water or methane. This again is in agreement with our experimenal observation that the exchange of methane for carbon monoxide, reaction 8, is very fast ($k^{abs} = (14 \pm 3) \times 10^{-10}$cm^3 mol^{-1} s^{-1}) and essentially irreversible. The reverse reaction 9 is not observed, and carbonyl once formed does not exchange with either water or methane.

Conclusions

Platinum cations Pt^+Ar_m, solvated with up to six inert argon atoms, were produced and their reactions with methane and methane-d_4 studied. While the bare Pt^+ ion dehydrogenates methane and forms a platinum−carbene complex Pt^+CH_2, the ion solvated with argon atoms can ligand exchange, forming a Pt^+CH_4 complex. In the ligand exchange up to four Ar atoms are evaporated for each CH_4 ligand. Reactions of the $m = 5$ and 6 clusters can also produce a Pt^+ArCH_4 cluster, which further exchanges to form the $Pt^+(CH_4)_2$ final product. Pt^+CH_4 is found to exchange the methane ligand in a strongly exothermic reaction for CO, while exchange with water is effectively thermoneutral. The exchange with CD_4 proceeds without any isotopic scrambling. The $Pt^+ + CH_4$ reaction path was reinvestigated in detail with the help of density functional (DFT) methods. These suggest that the dehydrogenation proceeds via a hydrido−methyl−platinum global minimum on the potential surface. The computed surface shows an almost negligible 2 kJ/mol barrier between the electrostatically bound Pt^+CH_4 complex and the inserted hydrido−methyl structure HPt^+CH_3. The lack of isotopic scrambling is explained by the inability of the $5d^86s$ Pt^+ ion with three unpaired electrons to simultaneously activate two CH bonds. The ligand exchange proceeds via a higher energy $Pt^+(CH_4)_2$ intermediate with two electrostatically bound methane ligands.

Acknowledgment. Financial support from the Deutsche Forschungsgemeinschaft and the Fonds der Chemischen Industrie is gratefully acknowledged.

References and Notes

(1) Halle, L. F.; Armentrout, P. B.; Beauchamp, J. L. *J. Am. Chem. Soc.* **1981**, *103*, 962.
(2) Georgiadis, R.; Armentrout, P. B. *J. Phys. Chem.* **1988**, *92*, 7067.
(3) Armentrout, P. B.; Beauchamp, J. L. *Acc. Chem. Res.* **1989**, *22*, 315.
(4) Buckner, S. W.; MacMahon, T. J.; Byrd, G. D.; Freiser, B. S. *Inorg. Chem.* **1989**, *28*, 3511.
(5) Perry, J. K.; Ohanessian, G.; Goddard, W. A., III. *Organometallics* **1994**, *13*, 1870.
(6) Irion, M. P.; Selinger, A. *Ber. Bunsen-Ges. Phys. Chem.* **1989**, *93*, 1408.
(7) Irikura, K. K.; Beauchamp, J. L. *J. Phys. Chem.* **1991**, *95*, 8344.
(8) Irikura, K. K.; Beauchamp, J. L. *J. Am. Chem. Soc.* **1991**, *113*, 2769.
(9) Lias, S. G.; Bartmess, J. E.; Liebman, J. F.; Holmes, J. L.; Levin, R. D.; Mallard, J. D. *J. Phys. Chem Ref. Data, Suppl.* **1988**, *17*, no. 1.
(10) Bigot, B.; Minot, C. *J. Am. Chem. Soc.* **1984**, *106*, 6601.
(11) Periana, R. A.; Taube, D. J.; Gamble, S.; Taube, H.; Satoh, T.; Fujii H. *Science* **1998**, *280*, 560.
(12) Heinemann, C.; Wesendrup, R.; Schwarz, H. *Chem. Phys. Lett.* **1995**, *239*, 75.
(13) Pavlov, M.; Blomberg, R. A.; Siegbahn, P. E. M.; Wesendrup, R.; Heinemann, C.; Schwarz, H. *J. Phys. Chem. A* **1997**, *101*, 1567.
(14) Caroll, J. J.; Weisshaar, J. C.; Siegbahn, P. E. M.; Wittborn, C. A. M.; Blomberg, M. R. A. *J. Phys. Chem.* **1995**, *99*, 14388.
(15) Albert, G.; Berg, C.; Beyer, M.; Achatz, U.; Joos, S.; Niedner-Schatteburg, G.; Bondybey, V. E. *Chem. Phys. Lett.* **1997**, *268*, 235.
(16) Berg, C.; Schindler, T.; Niedner-Schatteburg, G.; Bondybey, V. E. *J. Chem. Phys.* **1995**, *102*, 4870.
(17) Caravatti, P.; Allemann, M. *Org. Mass Spectrom.* **1991**, *26*, 514.
(18) Becke, A. D. *J. Chem. Phys.* **1993**, *98*, 5648.
(19) Lee, C.; Yang, W.; Parr, R. G. *Phys. Rev. B* **1988**, *37*, 785.
(20) Andrae, D.; Haeussermann, U.; Dolg, M.; Stoll, H.; Preuss, H. *Theor. Chim. Acta* **1990**, *77*, 123. Nicklass, A. Diplomarbeit, Universitaet Stuttgart, 1990.
(21) Gaussian 94, Revision D.4: Frisch, M. J.; Trucks, G. W.; Schlegel, H. B.; Gill, P. M. W.; Johnson, B. G.; Robb, M. A.; Cheeseman, J. R.; Keith, T.; Petersson, G. A.; Montgomery, J. A.; Raghavachari, K.; Al-Laham, M. A.; Zakrzewski, V. G.; Ortiz, J. V.; Foresman, J. B.; Cioslowski, J.; Stefanov, B. B.; Nanayakkara, A.; Challacombe, M.; Peng, C. Y.; Ayala, P. Y.; Chen, W.; Wong, W. W.; Andres, J. L.; Replogle, E. S.; Gomperts, R.; Martin, R. L.; Fox, D. J.; Binkley, J. S.; Defrees, D. J.; Baker, J.; Stewart, J. P.; Head-Gordon, M.; Gonzalez, C.; Pople, J. A. Gaussian, Inc., Pittsburgh, PA, 1995.
(22) Wesendrup, R.; Schroeder, D.; Schwarz, H. *Angew. Chem., Int. Ed. Engl.* **1994**, *33*, 3, 1174.
(23) Beyer, M.; Berg, C.; Albert, G.; Achatz, U.; Bondybey, V. E. *Chem. Phys. Lett.* **1997**, *280*, 459.
(24) Velegrakis, M.; Froudakis, G. E.; Farantos, S. C. *J. Chem. Phys.* **1998**, *109*, 4687.